Study of electrophoretic deposition of ZnO photoanodes on fluorine-doped tin oxide (FTO) glass for dye-sensitized solar cells (DSSCs)

V. F. Nunes[1]*, E. S. Teixeira[1], P. H. F. Maia Júnior[1], A. F. L. Almeida[2], F. N. A. Freire[1]
[1]Federal University of Ceará, Department of Materials Science and Engineering, 60440-554, Fortaleza, CE, Brazil
[2]Federal University of Ceará, Department of Mechanical Engineering, 60455-760, Fortaleza, CE, Brazil

Abstract

Semiconductors, such as zinc oxide (ZnO), are used in different scientific fields, including energy. This study applied ZnO thin films on a photovoltaic cell, specifically a dye-sensitized solar cell (DSSC). ZnO was used in solar cells due to its characteristics such as electronic mobility. Electrophoretic deposition (EPD) is an efficient method to deposit thin films since it can be done at room temperature and its parameters can be easily controlled. ZnO thin films were deposited on fluorine-doped tin oxide (FTO) glass, changing the tension parameter, and used in a DSSC, with different dye immersion times, between 7 and 24 h, to observe time effects on cell efficiency. For lower tension, 30 and 40 V, 7 h improved the cell efficiency, and at 50 V, 24 h favored the current density and efficiency. The highest efficiency was for the photoanode EPD deposited at 50 V, for 24 h dye immersion, at about 2.68%, and photocurrent of 13.55 mA/cm^2.
Keywords: zinc oxide, electrophoresis, DSSC, dye absorption, FTO glass.

INTRODUCTION

Titanium dioxide, tin oxide, and zinc oxide are some of the existing semiconductors materials with good photovoltaic performance. Besides, they can be used for other applications, such as gas sensors, catalysis, and batteries [1]. Zinc oxide (ZnO) has some characteristics that favor its use in photoanode of photovoltaic devices, such as a low band gap value (~3.3 eV), high electron mobility (115-155 cm^2), and morphological adaptability [2]. Another advantage of ZnO is the ability to be deposited on a substrate through a number of different methods, such as hydrothermal, sol-gel, chemical bath, electrophoresis, among many others. Electrophoretic deposition (EPD) is a method where two electrodes in parallel are immersed in a colloidal solution electrically charged, where the particles flow in the direction of the electrode of opposite charge through the application of an external voltage [3]. The tension and the deposition time are some of the main parameters of the EPD deposition; others can be listed, such as the solvent for the suspension, viscosity, and inter-electrode distance [3]. The electrophoretic deposition method brings forward advantages such as low cost, the ability of thickness control, simple set-up, and a high rate of production [4]. The thickness produced ranges from a few micrometers to millimeters; it can create a dense layer of the ceramic material on a conductive substrate. EPD can be applied in a variety of shapes and sizes [5]. Fig. 1 illustrates a scheme of electrophoretic deposition of semiconductors. The dye has an important play in the DSSC structure, acting as a sensitizer, by transferring the electron to the working electrode. The sunray reaches the dye through the fluorine-doped tin oxide (FTO) and generates electrons, which pass to the ZnO films with a porous structure that absorbs the dye. For this reason, the applied dye has to be properly absorbed by the zinc oxide nanostructure [6].

The loading of the dye should not cause aggregation that blocks the efficiency of the cell [7]. Finding the perfect timing for the dye loading is essential to avoid those particle

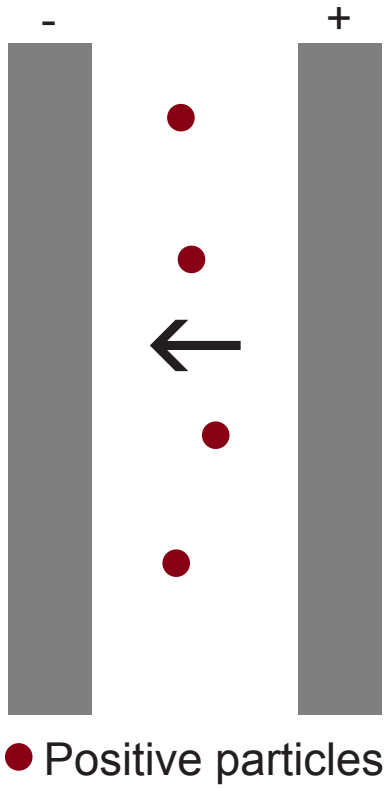

Figure 1: Scheme of the EPD mechanism.

*vanjafnunes@gmail.com
https://orcid.org/0000-0003-2458-5616

aggregates without lowering the charging of the excited dye electrons; it is necessary to adjust such a time that causes a balance between those two factors, reducing the formation of aggregates that increase resistance inside the cell and, at the same time, cover the surface of the semiconductor layer, avoiding losses of charge transfer between the film and the dye. Also, the optimum dye loading can vary according to the thickness of the film; in this work, it was changed by the applied tension in EPD, which affects the electron diffusion length inside the cell [8]. This work tries to find this balance and the dye immersion time that is more effective for different tension values, especially combining the EPD method and zinc oxide. Most works that change the dye loading time focus on titanium dioxide polymorphs, rutile and anatase [8, 9]. Other researches focus on techniques such as co-precipitation [10], hydrothermal growth [11, 12], magnetron sputtering [13], doctor blade [14], and screen printing [15]. Another factor that reduces significantly the PCE (photocurrent efficiency) is the charge recombination inside the cell between the photoanode/dye surface or the dye/electrolyte surface; therefore, to improve the cell's efficiency it is necessary to create a pathway from the charge carriers to the charge collectors, avoiding electron recombination [16].

In this work, the external tension applied between the electrodes was changed three times to observe the effects of this parameter on the photovoltaic behavior of the zinc oxide. Additionally, the dye absorption time of the semiconductor layer, 7 and 24 h, was also changed to analyze the effects of dye absorption on dye solar cell efficiency. This paper aims to find the optimum combination between dye loading time and external tension applied for the EPD deposition to improve the photovoltaic efficiency of zinc oxide. Besides, it tries to demonstrate the viability of the electrophoretic deposition, showing that it can produce uniform films with efficiency for photoanodes, close to those produced by more used methods, such as doctor blade, screen printing, and hydrothermal growth.

EXPERIMENTAL

Thin films of zinc oxide were deposited on FTO (fluorine-doped tin oxide, Solaronix) glass by electrophoretic deposition (EPD, k33-300V, Kasvi). The glass presented sheet resistivity of about 28 ohm/sq. The set-up was a counter electrode of platinum (positive), an electrode of FTO (negative), and the colloidal solution of a commercial zinc oxide powder in ethanol (8 g/L), as described elsewhere [17]. The parameters of deposition were 30, 40, and 50 V for 5 min each. The ZnO was diluted on an ethanol solution at the concentration of 8 g/L, with 0.1 g/L of magnesium nitrate to help create the charged particles on the surface of the electrodes. The solutions were previously treated in ultrasonic baths for 30 min with acetone, ethanol, and distilled water, before being used in the electrophoresis process. After being deposited on FTO, the ZnO films were thermally treated at 450 °C for 40 min. The film's area was 0.25 cm^2. All reagents were used without further purification.

After deposition, the conductive glass was used as a photoanode in a dye-sensitized solar cell (DSSC) to obtain the photovoltaic behavior of the ZnO thin films and the effects of the tension values of EPD on parameters such as current density and photovoltaic efficiency. Moreover, the time of dye absorption for the films was 7 and 24 h to study its possible effects on cell efficiency. Other reagents used to assemble the DSSC were iodide/triiodide electrolyte ($3I^-/I^-_3$, Iodolyte AN-50, Solaronix, Switzerland), ruthenium-based dye (N719, Solaronix), with isopropyl alcohol at the concentration of 0.0003 M acting as a solvent, and platinum as a counter electrode. The platinum used as the counter electrode (CE) was purchased from Solaronix with a resistance of around 18 ohm/cm^2. After the illumination simulations, the J-V (current density vs. tension/voltage) curves were plotted and the efficiencies of the cells were calculated by the equations found elsewhere [18]. The UV-vis spectroscopy (Cary Series, Agilent Techn.) measurements were performed between 200 and 800 nm. The morphological characterization of the films was done through X-ray diffraction (XRD, DMAXB, Rigaku) with CuKα radiation. The J-V tests were done on a potentiostat (Autolab PGSTAT302N, Metrohm) under 100 mW/cm^2 illuminations, within the spectrum range of incident light radiation corresponding to 0, 0.033, 0.067, and 0.1 W/cm^2 and LED white neutral lamp used for the simulation. Scanning electron microscopy (SEM) was done with a microscope (Quanta 450 FEG, FEI).

RESULTS AND DISCUSSION

SEM analysis: Fig. 2 shows the scanning electron micrographs at a high magnification of the zinc oxide films deposited at 30 V (Fig. 2a), 40 V (Fig. 2b), and 50 V (Fig. 2c). The film constructed at 50 V seemed to be more porous, which can help to explain the longer time needed for the dye absorption. The porosity in the three films was a characteristic of the ethanol used as a solvent for the zinc oxide solution, as pointed out by Hasanpoor et al. [17]. Similarly, Hossein-Babaei et al. [19] observed three-dimensional shaped geometric structures of the ZnO deposited by electrophoresis between 10 and 60 V. These shapes were more clearly visualized in the microstructure of 50 V EPD film.

X-ray diffraction characterization: in the XRD patterns, the peaks were indexed for the ZnO phase (ICSD file 29272) for the three samples (Fig. 3). Through the Scherrer equation, the crystallite size (D) was calculated: $D=k.\lambda/(\beta.\cos\theta)$, where k was taken as 0.9, λ is the wavelength (1.5406 Å), β is the broadening of the diffraction line (full width at half maximum), and θ is the Bragg's diffraction angle [20]. This equation estimated the average ZnO particle size. For the film deposited at 30 V, the average size (D) was found to be 120.8 nm; for the 40 V EPD, the average crystallite size was 119.7 nm and, for 50 V, D was 116.8 nm. The viscosity of the ethanol solvent (0.001074 Pa.s) can explain the decrease in the particle size from 30 to 40 to 50 V [17]. Optimum

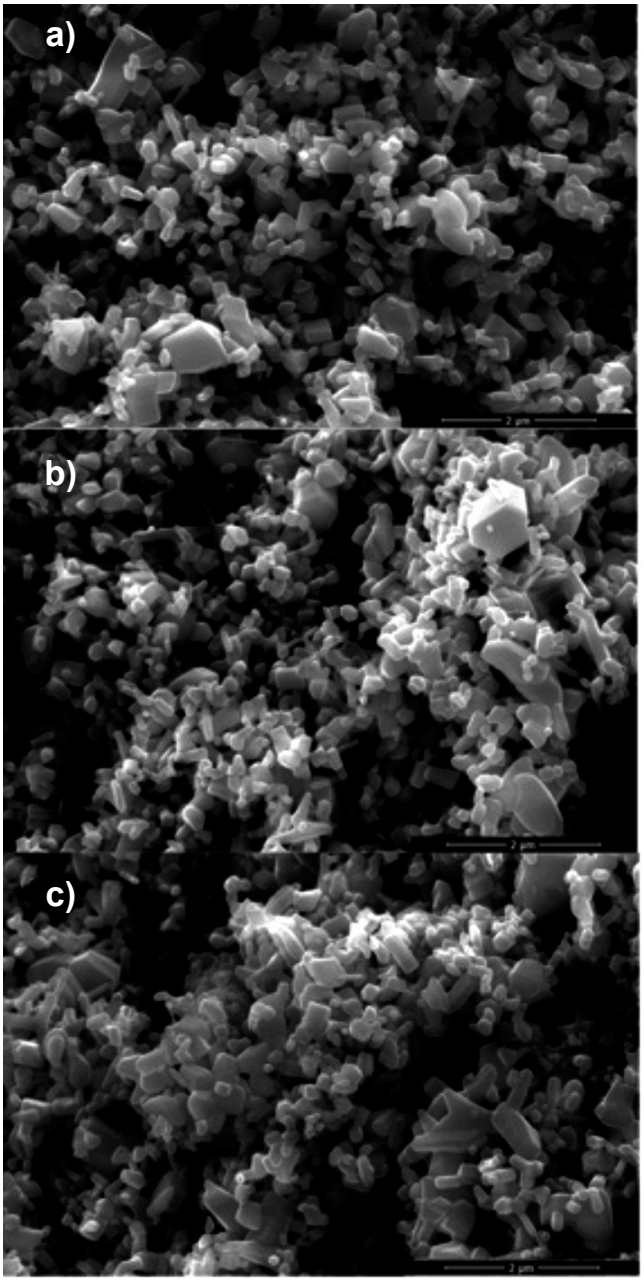

Figure 2: SEM images of the EPD films deposited at: a) 30 V; b) 40 V; and c) 50 V.

crystallite size is very crucial to the dye absorption process; according to Arka et al. [21], small particle sizes are good dye absorbers but poor charge carriers and larger particles are poor dye absorbers but good charge carriers. The particles found in this work can be classified as large particles. The characteristic peaks of the zinc oxide were present in the patterns, (100), (002), and (101), matching the wurtzite structure of the zinc oxide. The more prominent one was the (101) peak for the three cases. According to Xue et al. [22], the reduction of the (002) peak intensity may indicate the formation of nanosheets in the structure. The remaining peaks were characteristics of the tin oxide on the FTO conductive glass: at 26.5°, the peak (110); at 33° peak (101); at 37° (200); at 51° (211); and at 61° (310).

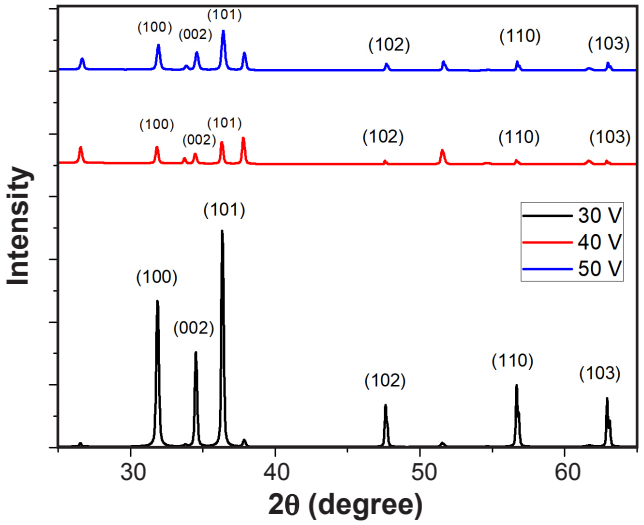

Figure 3: XRD patterns of the EPD photoanodes at three voltages.

UV-vis spectroscopy characterization: through the analysis of the absorbance spectra in Fig. 4a, all absorption peaks' wavelength ranges were between approximately 350 and 400 nm, following which was verified by Kannan et al. [23], who synthesized ZnO nanorods on FTO. By increasing the voltage, there was a red shift on the absorbance values, highlighting the 50 V zinc oxide thin film, with a peak at approximately 360 nm wavelength. This shift contributed to a better performance of the cell assembled with the photoanode of ZnO deposited at 50 V. In Fig. 4b, the transmittance data shows the highest values for the 30 V EPD deposited zinc oxide film. This matched the values for absorbance, where the film with the lowest absorbance had higher transmittance. The method described in [24] was used to calculate the band gap values (E_g) by extrapolating the best linear fit, resulting in the values of approximately 3.85, 3.16, and 2.8 eV for the 30, 40, and 50 V EPD deposited films, respectively (Fig. 5).

Dye-absorption studies: by the data observed in the graphs of Fig. 6 and listed in Table I, an improvement in the efficiency was driven by the increase of the current density. The current density of the cell was higher (13.55 mA/cm^2) for the 50 V EPD, which favored a better photovoltaic efficiency. This can be due to the fact that at 50 V the ZnO particle size increased and improved the charge transportation [21]. Consequently, more electrons were excited from the dye to the photoanode and external circuit. This result agreed with another study [17], which verified an increase of 39% of deposited zinc oxide nanoparticles when using ethanol as solvent at higher voltages. The open-circuit voltages (V_{oc}) were close in values, due to the fact that the DSSC had the same composition (Pt CE and same dye) [25]. Moreover, for the same voltage, 7 h was not enough to absorb the dye into the photoanodes, significantly reducing the short-circuit current density (J_{sc}) to 0.05 mA/cm^2, representing a decrease of 99.6%. Lower absorption caused regions of bare ZnO surface, which caused charge recombination by back electron transfer that led to decreased J_{sc} and V_{oc} [26]. On

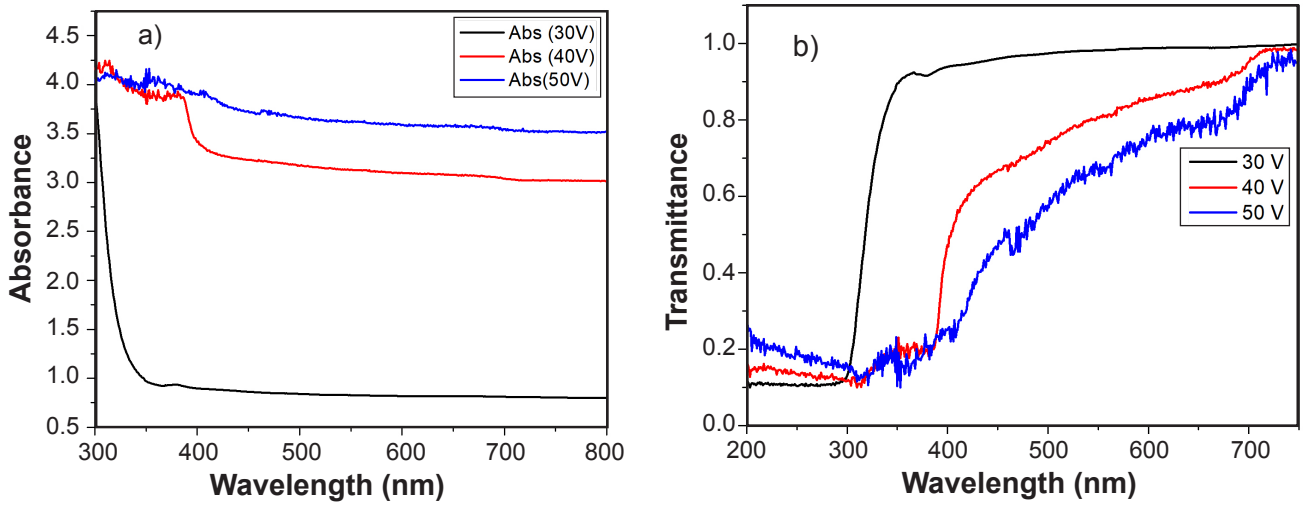

Figure 4: Absorbance (a) and transmittance (b) spectra for the photoanodes prepared at 30, 40, and 50 V deposition parameter.

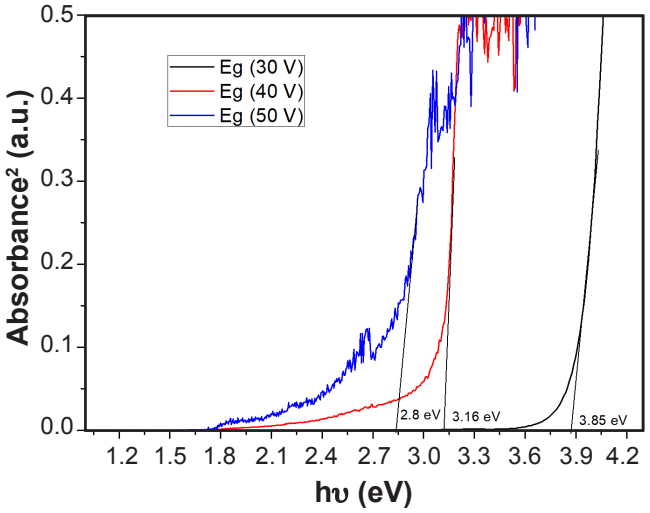

Figure 5: Absorbance plot to estimate band gap values.

the other hand, less time favored the current density at 30 and 40 V. The photocatalytic tests revealed higher J_{sc} for 7 h dye absorption at these voltages. Consequently, the higher current densities helped the improvement of efficiency for 7 h dye absorption at 30 and 40 V.

Table I also shows that for the 24 h dye immersion, at the 30 and 40 V, the series resistance (R_s) increased, which can be caused by the creation of an insulating layer near the surface of the photoanode [4]. This resistance helped to decrease the photocurrent of the cell. The parallel resistance (R_{sh}) was higher for lower efficiency values. Also, at these voltages, for 24 h, the short-circuit current density values indicated low electron injection efficiency, which was observed elsewhere [27]. Šulčiūtė et al. [28] state that when ZnO is deposited by EPD, non-active layers can be formed near the surface, where the UV light is not efficiently irradiated. Chou et al. [29] also affirm that ZnO is more affected by

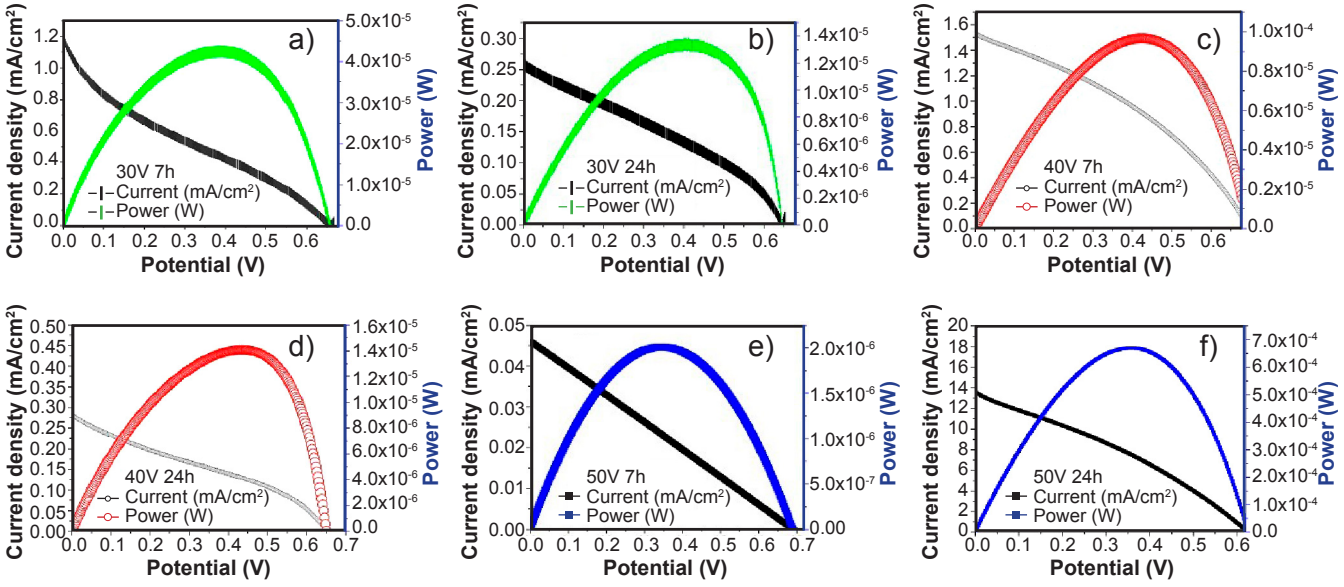

Figure 6: J-V curves for the EPD deposited ZnO thin films at: a) 30 V/7 h; b) 30 V/24 h; c) 40 V/7 h; d) 40 V/24 h; e) 50 V/7 h; and f) 50 V/24 h.

Table I - Parameters of current-voltage obtained from DSSC of the tested ZnO photoanodes.

Conditions*		J_{sc} (mA/cm²)	FF	Efficiency (%)	V_{oc} (V)	R_s (ohm/cm²)	R_{sh} (ohm/cm²)
30 V	7 h	1.17±0.35	0.22±0.01	0.17±0.05	0.66±0.02	347.5±0.9	302.0±0.6
	24 h	0.26±0.03	0.32±0.01	0.05±0.01	0.64±0.05	553.3±0.1	2887.8±0.3
40 V	7 h	1.53±0.32	0.49±0.06	0.52±0.12	0.70±0.04	17.3±0.9	826.8±0.7
	24 h	0.28±0.02	0.31±0.02	0.06±0.02	0.65±0.02	651.35±0.02	2074.61±0.02
50 V	7 h	0.05±0.01	0.25±0.01	0.010±0.002	0.69±0.01	14818.3±0.1	15290±1
	24 h	13.5±0.9	0.32±0.01	2.68±0.13	0.626±0.004	25.7±0.3	58.1±0.8

** EPD voltage and time of dye absorption.*

conditions of dye loading, therefore different values of efficiency are observed when changing the dye loading time, caused by the interactions between the nanoparticles of ZnO and dye, forming aggregates that can affect current density values. The low values for the fill factor for all the cells indicated a higher rate of recombination between the charge carriers of the photoanode and the electrolyte $3I^-/I_3^-$ [25]. In a DSSC, there is a kinetic competition between the electrons transported through the semiconductor layer and the ones which recombine with the electrolyte pair. To increase the photocurrent density, the movement of electrons to go through the ZnO semiconductor must be faster than the recombination reaction, in an order of milliseconds, otherwise, the photocurrent drops significantly, reducing the efficiency of the cell [30]. A pathway must be created from the photoinduced charge carriers to the current collector to minimize the recombination in the ZnO-dye and the electrolyte-dye interfaces [16].

In Table II, the efficiency of ZnO-based solar cells tested in this work, specifically the one with the highest efficiency, ZnO at 50 V and 24 h dye absorption, and solar cells based on ZnO produced through different methods of deposition are listed. It is possible to observe that the electrophoresis method can achieve higher efficiency than other methods such as sol-gel and doctor blade. Doctor-blade and screen-printing methods are very popular due to their economic aspect; however, they face problems of reproducibility, inhomogeneity, and surface topography [21]. Therefore, electrophoresis becomes a real and viable alternative for the synthesis of thin films, by showing good results, close or higher than the ones achieved by the most common methods.

Table II - Comparing efficiency between ZnO solar cells from this work and references.

Efficiency (%)	Ref.
2.68	This work
1.77	[31]
0.89	[18]
1.16	[14]
2.08	[32]
2.26	[25]

CONCLUSIONS

The electrophoretic method successfully deposited zinc oxide on fluorine-doped tin oxide (FTO). The semiconductor deposited by electrophoretic deposition (EPD) produced photovoltaic activity determined by J-V measurements on dye-sensitized solar cells (DSSCs). The solar cell with the best results, between those tested, was the one that used the ZnO deposited at 50 V and 24 h of dye absorption, with the best results of current density, 13.55 mA/cm², and efficiency, 2.68%. These results indicated that electrophoresis is a viable alternative to the production of homogeneous and crystalline semiconductors that can be applied to assemble solar cells, compared with methods widely used such as doctor-blade and screen printing.

ACKNOWLEDGMENTS

The authors would like to acknowledge the Brazilian research agency Coordenação de Aperfeiçoamento de Pessoal de Nível Superior-Capes for the financial support, and the Laboratório de Filmes Finos e Energias Renováveis-LAFFER for the assistance throughout the research. The authors would like to thank the Central Analítica-UFC (funded by Finep-CT-INFRA, CAPES-Pró-Equipamentos, and MCTI-CNPq-SisNano2.0) for microscopy measurements.

REFERENCES

[1] B. Praveen, K. Pugazhendhi, J.S.S. Mary, S. Padmaja, E.M. Arnold, J. Madhavan, J.M. Shyla, Mater. Today Proc. **8** (2019) 239.
[2] F. Lai, J. Yang, Y. Hsu, S. Kuo, J. Colloid Interface Sci. **562** (2020) 63.
[3] S. Obregón, G. Amor, A. Vázquez, Adv. Colloid Interface Sci. **269** (2019) 236.
[4] E. Mohammadi, M. Aliofkhazraei, A. Sabour Rouhaghdam, Ceram. Int. **44** (2018) 1471.
[5] J.L. Pantoja-Pertegal, A. Díaz-Parralejo, A. Macías-García, J. Sámchez-González, E.M. Cuerda-Correa, Ceram.

Int. **47** (2021) 13312.
[6] S.V. Kumar, H.Y. Goudar, K.A. Razak, H.K. Madhusudhana, A. Buradi, A. Afzal, C.A. Saleel, Mater. Today Proc. **47** (2021) 6153.
[7] A. Roy, S. Sundaram, T.K. Mallick, Chem. Phys. Lett. **776** (2021) 138688.
[8] F.M. Rajab, J. Nanomater. **2016** (2016) 1.
[9] M.K. Hossain, M.F. Pervez, M.N.H. Mia, A.A. Mortuza, M.S. Rahaman, M.R. Karim, J.M.M. Islam, F. Ahmed, M.A. Khan, Results Phys. **7** (2017) 1516.
[10] S. Selvinsimpson, P. Gnanamozhi, V. Pandiyan, M. Govindasamy, M.A. Habila, N. AlMasoud, Y. Chen, Environ. Res. **197** (2021) 111115.
[11] K.A. Salazar, V.C. Agulto, M. John, F. Empizo, K. Shinohara, K. Yamanoi, T. Shimizu, N. Sarukura, A.C.C. Yago, P. Kidkhunthod, S. Sattayaporn, V.A.I. Samson, R.V. Sarmago, J. Cryst. Growth **574** (2021) 126332.
[12] S. Aksoy, K. Gorgun, Y. Caglar, M. Caglar, J. Mol. Struct. **1189** (2019) 181.
[13] S. Limwichean, N. Kasayapanand, C. Ponchio, H. Nakajima, V. Patthanasettakul, P. Eiamchai, G. Meng, M. Horprathum, Ceram. Int. **47**, 24 (2021) 34455.
[14] S. Khadtare, H.M. Pathan, S. Han, J. Park, J. Alloys Compd. **872** (2021) 159722.
[15] W.-C. Chang, C.-H. Lee, W.-C. Yu, Nanoscale Res. Lett. **7** (2012) 688.
[16] K.B. Bhojanaa, M. Ramesh, A. Pandikumar, Mater. Res. Bull. **122** (2020) 110672.
[17] M. Hasanpoor, M. Aliofkhazraein, D.H. Hami, Ceram. Int. **42** (2016) 6906.
[18] S. Suresh, A. Pandikumar, S. Murugesan, R. Ramaraj, S.P. Raj, Mater. Express **1** (2011) 307.
[19] F. Hossein-Babaei, M. Ghalamboran, E. Yousefiazari, Mater. Lett. **209** (2017) 404.
[20] M. Thirumoorthi, J.T.J. Prakash, Mater. Sci. Eng. B **248** (2019) 114402.
[21] G.N. Arka, S.B. Prasad, S. Singh, Sol. Energy **226** (2021) 192.
[22] B. Xue, Y. Liang, L. Donglai, N. Eryong, S. Congli, F. Huanhuan, X. Jingjing, J. Yong, J. Zhifeng, S. Xiaosong, Appl. Surf. Sci. **257** (2011) 10317.
[23] S. Kannan, N.P. Subiramaniyam, S.U. Lavanisadevi, Mater. Lett. **274** (2020) 127994.
[24] C. Sandoval, O. Marin, S. Real, D. Comedi, M. Tirado, Mater. Sci. Eng. B **187** (2014) 21.
[25] X. Chen, Y. Tang, W. Liu, Molecules **22** (2017) 1284.
[26] A. Roy, S. Sundaram, T.K. Mallik, Chem. Phys. Lett. **776** (2021) 138688.
[27] E.J. Canto-Aguilar, M. Rodríguez-Pérez, R. García-Rodríguez, F.I. Lizama-Tzec, A.T.D. Denko, F.E. Osterloh, G. Oskam, Electrochim. Acta **258** (2017) 396.
[28] A. Šulčiūtė, S. Ostachavičiūtė, E. Valatka, Chemija **28** (2017) 85.
[29] T.P. Chou, Q. Zhang, G. Cao, J. Phys. Chem. C **111** (2007) 18804.
[30] J.E. Ikepsu, S.E. Iyuke, M. Daramola, O.A. Oyetunde, Sol. Energy **206** (2020) 918.
[31] A.S. Mary, K.B. Bhojanaa, P. Murugan, A. Pandikumar, J. Alloys Compd. **888** (2021) 161439.
[32] M. Sufyan, U. Mehmood, Y.Q. Gill, R. Nazar, A.U.H. Khan, Mater. Lett. **297** (2021) 130017.
(Rec. 23/07/2021, Rev. 14/09/2021, 09/10/2021, Ac. 13/10/2021)